



ELSEVIER

Comput. Methods Appl. Mech. Engrg. 136 (1996) 225–258

**Computer methods
in applied
mechanics and
engineering**

A unified approach for parameter identification of inelastic material models in the frame of the finite element method

Rolf Mahnken*, Erwin Stein

Institut für Baumechnik und Numerische Mechanik, University of Hannover, Appelstrasse 9a, D-30167 Hannover, Germany

Received 3 March 1995; revised 22 November 1995

Abstract

This work is concerned with identification of parameters for inelastic material models. In order to account for possible non-uniformness of stress and strain distributions, the identification is performed in the frame of the finite element method. In particular, linearization procedures are described in a systematic manner for the case of complex material models within a geometric linear theory. This unified approach allows one to apply the Newton method for solving the associated direct problem and to apply gradient based methods for solving the associated inverse problem, which is considered as an optimization problem. Two numerical examples demonstrate the versatility of our approach: firstly, we consider Cooks membrane problem based on simulated data for re-identification of material parameters for a viscoplastic power law. Furthermore, material data for J_2 -flow theory are determined, based on experimental data obtained by a grating method for a compact specimen, and we will investigate the results by using different starting values and stochastic perturbation of the experimental data.

1. Introduction

The study of inelastic material behaviour is usually made in two steps: Firstly, a mathematical model is formulated with regards to the physical effects thus considering steady state creep, relaxation, cycling hardening and softening, Bauschinger effect, temperature and damage effects, etc. (see e.g. [1, 2]). Then identification of the material constants based on experimental data becomes necessary, which in the mathematical terminology is an inverse problem (see e.g. [3–5]).

Concerning experimental issues the type of test and the choice of the sample are most important. The classical characteristic tests, e.g. creep, relaxation or cyclic tests, are essentially conducted in simple tension, or tension-compression at constant temperature. The sample, e.g. a cylindrical hollow specimen, is subjected to an axial load (force or displacement), which produces strains and stresses assumed to be *uniform* within the whole volume of the specimen. Various publications exist in the literature based on this conception [1, 2, 6–9]. However, as noted in [1, p. 77], to achieve uniformness for stresses, strains and temperature is ‘one of the difficulties of mechanical testing for the characterization of materials’. In nearly all mechanical tests, deformations eventually cease to be uniform due to localization, fracture and other failure mechanisms. Furthermore, non-uniformness is unavoidable in the case of necking of the sample in tension tests or barreling due to friction of the sample in compression tests.

So far, to the authors knowledge, very few publications exist in the literature in order to account for non-uniform stress and strain distribution [10–12] during the experiment. The purpose of this work is

*Corresponding author.

to present a unified strategy for parameter identification which accounts for this inhomogeneity. When considering complex structures, such as a plate with a hole, the incorporation of non-uniform stresses and strains requires the solution of field equations. For this reason we will consider parameter identification in the context of the finite-element method (FEM).

Considering the solution of the associated inverse problem, various strategies exist in the literature. In recent years neural networks—derived through a modeling of human brain—become attractive tools. Application of neural networks for parameter identification of visco plastic material models is reported in [13].

A common—classical—approach for solution of the inverse problem is to consider parameter identification as an *optimization problem*. In this respect a least-squares functional is minimized in order to provide the best agreement between experimental data and simulated data in a specific norm (optimal approach strategy). In order to stabilize the numerical results it may be necessary to amend this basic function by a regularization term. In the context of identification for visco-plastic material models, this issue was discussed in [7, 8] and stabilization was achieved by using model information of the specific material law. Furthermore, let us mention that, when considering parameter identification in the context of the finite element method, this approach is similar to procedures in shape optimization. In the corresponding terminology the material parameters are the *design variables* of the optimization problem (see e.g. [14]).

Algorithms for solution of the resulting optimization problem, basically, may be classified into two classes, i.e. methods which only need the value of the least-squares function (zero-order methods) and descent methods, which require also the gradient of the least-squares function (first-order methods). In [8, 12] two specific algorithms of the above classes, i.e. an evolutionary strategy due to Schwefel [15] and a projection algorithm due to Bertsekas [16] were compared, and as a main result the latter proved to be much more efficient. For this reason a gradient based method is applied in this work for minimization of the objective function of least-squares type.

This paper is structured as follows: In the next section the basic equations for the direct problem and the inverse problem for modeling inelastic material behaviour are summarized. In Section 3, firstly, we give a short review for solution of the discretized direct problem in the context of the finite element method for geometric linear problems. Furthermore, for complex material laws, we present a unified concept for linearization of the associated functions in the local iteration procedure. Then, by simple condensation local tangent moduli are derived. This condensation can be performed, both directly, e.g. by use of a Gaussian factorization and in many cases analytically. We will show how this strategy is easily extended to plane stress problems. Furthermore, we discuss the relation of the local tangent moduli to the tangent modulus of the global iteration procedure. Section 4 is concerned with a solution strategy for the inverse problem. Here, basically, we show that the same conception as for determination of the global tangent modulus of Section 3 can be applied in the sensitivity analysis for determination of the gradient of the least-squares functional by exploiting the structure of the local tangent moduli. Two numerical examples are presented in Section 5: In the first example the proposed algorithm is tested by re-identifying parameters of a viscoplastic power law based on simulated data for Cooks membrane problem. The next example is based on experimental data for a compact tension specimen. Here, parameters are identified for J_2 -flow theory with non-linear isotropic hardening, thus yielding to very good agreement between numerical simulation and experimental observations obtained by a grating method. Furthermore, in this example the effect of using different starting vectors and the effect of perturbation of the data on the material parameters will be discussed.

2. Basic equations

Let $\mathcal{I} = [0, T]$ be the time interval of interest and let $\Omega \subset \mathbb{R}^{n_{\text{dim}}}$ be the reference placement of a body \mathcal{B} under consideration with smooth boundary $\partial\Omega$, where $n_{\text{dim}} = 1, 2, 3$ is the spatial dimension of the problem. Then, any material point $P \in \mathcal{B}$ is defined by $\mathbf{x}(P) \in \Omega$. In addition, $\mathbf{u} \in U: \Omega \times \mathcal{I} \rightarrow \mathbb{R}^{n_{\text{dim}}}$ denotes the displacement field, and $\boldsymbol{\varepsilon}, \boldsymbol{\sigma}: \Omega \times \mathcal{I} \rightarrow \mathcal{S}$ denote the actual strain and stress fields,

respectively, where \mathcal{S} is the space of symmetric rank-two tensors.

We shall denote by $\hat{\mathbf{u}}$ the prescribed boundary displacement on $\partial\Omega_u$ and designate by $\hat{\mathbf{t}}$ the prescribed boundary traction vector on $\partial\Omega_\sigma$. Furthermore, $\hat{\mathbf{b}}$ denotes the body force per unit volume. As usual we assume $\partial\Omega_u \cup \partial\Omega_\sigma = \partial\Omega$ and $\partial\Omega_u \cap \partial\Omega_\sigma = \emptyset$.

In the context of a small strain theory the total strain field $\boldsymbol{\varepsilon}$ is obtained from the displacement field \mathbf{u} via

$$\boldsymbol{\varepsilon} = \frac{1}{2} \left((\text{grad } \mathbf{u})^\top + \text{grad } \mathbf{u} \right), \tag{1}$$

and an additive split into an elastic part and an inelastic part is assumed, i.e.

$$\boldsymbol{\varepsilon} = \boldsymbol{\varepsilon}^{\text{el}} + \boldsymbol{\varepsilon}^{\text{in}}. \tag{2}$$

2.1. Constitutive equations in plasticity

In addition to the above relations, for classical infinitesimal plasticity the following assumptions are common practice (see e.g. [1, 19]):

- (1) A convex elastic domain \mathbb{E} is defined in the simplest case by a smooth (single surface) yield criterion in stress space, i.e.

$$\mathbb{E} := \{ (\boldsymbol{\sigma}, \boldsymbol{\xi}) \in \mathcal{S} \times \mathbb{R}^{n_q} : \Phi(\boldsymbol{\sigma}, \boldsymbol{\xi}) \leq 0 \}, \tag{3}$$

where \mathbb{R}^{n_q} is a suitable vector space of n_q stress-like internal variables $\boldsymbol{\xi}$ (internal forces). Then, in classical plasticity states $(\boldsymbol{\sigma}, \boldsymbol{\xi})$ outside \mathbb{E} are non-admissible.

- (2) A free energy function $\Psi(\boldsymbol{\varepsilon}^{\text{el}}, \mathbf{q})$ is assumed, where \mathbf{q} denotes the vector of strain-like internal variables.
- (3) The stress-like internal variables $\boldsymbol{\xi}$ are defined to be conjugate to the strain-like internal variables \mathbf{q} in the sense that $\boldsymbol{\xi} := \rho \partial\Psi/\partial\mathbf{q}$, where ρ denotes the material density which will assumed to be constant.

Then, for the case of *associated* plasticity, the principle of maximum dissipation yields the following relations for the stress strain conditions, the evolution equations for inelastic strains and the strain-like internal variables and the loading and unloading conditions, respectively (see [19]):

$\boldsymbol{\sigma} = \rho \frac{\partial\Psi(\boldsymbol{\varepsilon}^{\text{el}}, \mathbf{q})}{\partial\boldsymbol{\varepsilon}^{\text{el}}}, \quad \boldsymbol{\xi} = \rho \frac{\partial\Psi(\boldsymbol{\varepsilon}^{\text{el}}, \mathbf{q})}{\partial\mathbf{q}}$ $\dot{\boldsymbol{\varepsilon}}^{\text{in}} = \gamma \frac{\partial\Phi(\boldsymbol{\sigma}, \mathbf{q})}{\partial\boldsymbol{\sigma}} \quad \dot{\mathbf{q}} = -\gamma \frac{\partial\Phi(\boldsymbol{\sigma}, \boldsymbol{\xi})}{\partial\boldsymbol{\xi}}$ $\gamma \geq 0, \quad \Phi(\boldsymbol{\sigma}, \boldsymbol{\xi}) \leq 0, \quad \gamma\Phi(\boldsymbol{\sigma}, \boldsymbol{\xi}) = 0$	$\tag{4}$
--	-----------

For the particular case of J_2 -flow theory with isotropic hardening, we choose $(\boldsymbol{\sigma}, \boldsymbol{\xi}) = (\boldsymbol{\sigma}, R)$ and $(\boldsymbol{\varepsilon}^{\text{in}}, \mathbf{q}) = (\boldsymbol{\varepsilon}^{\text{in}}, e)$, where e models the isotropic hardening and R measures the radius of the yield surface in the space of deviatoric stresses. Furthermore, we set

$$\rho\Psi(\boldsymbol{\varepsilon}^{\text{el}}, e) := \frac{1}{2} \boldsymbol{\varepsilon}^{\text{el}} : \mathbf{C}\boldsymbol{\varepsilon}^{\text{el}} + W(e)$$

$$\mathbf{C} := 2\mu\mathbf{I} + \lambda\mathbf{1} \otimes \mathbf{1} \tag{5}$$

$$W(e) := q \left(e + \frac{1}{b} \exp(-be) - \frac{1}{b} \right)$$

$$\Phi(\boldsymbol{\sigma}, R) := \sigma_v(\boldsymbol{\sigma}) - (\sigma_0 + R)$$

in order to specify the state potential and the yield function, respectively. Here, we used the notation

$$\sigma_v(\boldsymbol{\sigma}) = \left[\frac{3}{2} \boldsymbol{\sigma}' : \boldsymbol{\sigma}' \right]^{1/2}, \quad \boldsymbol{\sigma}' = \mathbf{D}\boldsymbol{\sigma}, \quad \mathbf{D} = \mathbf{I} - \frac{1}{3} \mathbf{1} \otimes \mathbf{1} \tag{6}$$

for the second invariant $\sigma_v(\boldsymbol{\sigma})$ and the deviatoric stress tensor $\boldsymbol{\sigma}'$, respectively. Furthermore, in Eq. (5) \mathbf{C} is the elasticity tensor with Lamé constants μ , and λ , and $\mathbf{1}$ and \mathbf{I} denote the second- and fourth-order unit tensor, respectively.

Consequently, due to the above particular choices the elastic part in Eq. (2) is obtained from

$$\boldsymbol{\varepsilon}^{el} = \mathbf{C}^{-1} \boldsymbol{\sigma}, \tag{7}$$

whilst the inelastic part—for the case of associative plasticity with isotropic hardening—is represented by the following set of equations:

$$\begin{aligned} \dot{\boldsymbol{\varepsilon}}^{in} &= \frac{3}{2} \gamma \mathbf{n}, & \mathbf{n} &:= \frac{1}{\sigma_v(\boldsymbol{\sigma})} \boldsymbol{\sigma}' \\ \Phi(\boldsymbol{\sigma}, R) &= \sigma_v(\boldsymbol{\sigma}) - (\sigma_0 + R) \\ R &= \hat{R}(e) = q(1 - \exp(-be)) \\ \dot{e} &= \gamma \\ \gamma &\geq 0, & \Phi(\boldsymbol{\sigma}, q) &\leq 0, & \gamma \Phi(\boldsymbol{\sigma}, q) &= 0 \end{aligned} \tag{8}$$

REMARKS

- (1) Observe that the vector $\boldsymbol{\kappa} := [\sigma_0, b, q]^T$ defines the set of $m = 3$ material parameters of the above model related to the inelastic material behaviour.
- (2) Note, that Eq. (8)₃ may also be obtained by integration of the following evolution law [21]

$$\dot{R} = b(q - R)\dot{e}. \tag{9}$$

- (3) For the case of *linear hardening* Eq. (8)₃ is replaced by

$$R = He, \tag{10}$$

such that $\boldsymbol{\kappa} := [\sigma_0, H]$ defines the set of $m = 2$ material parameters.

2.2. Constitutive equations in visco-plasticity

Concerning the elastic part in Eq. (2), as before, we will assume that Eq. (7) is also valid for problems in visco-plasticity. The inelastic part in general is characterized by a set of evolution equations for the inelastic strains accompanied by a set of evolution equations for n_q internal variables $\mathbf{q} \in \mathbb{R}^{n_q}$, which may be scalar or tensor valued functions

$$\begin{aligned} \dot{\boldsymbol{\varepsilon}}^{in} &= f(\boldsymbol{\sigma}, \mathbf{q}, \boldsymbol{\xi}, \Theta, \boldsymbol{\varepsilon}^{in}, \dots; \boldsymbol{\kappa}) \\ \dot{\mathbf{q}} &= g(\boldsymbol{\sigma}, \mathbf{q}, \boldsymbol{\xi}, \Theta, \boldsymbol{\varepsilon}^{in}, \dots; \boldsymbol{\kappa}) \end{aligned} \tag{11}$$

From the above equations it can be seen, that, typically these relations may also depend on the stresses $\boldsymbol{\sigma}$, some dual variables $\boldsymbol{\xi}$, the temperature Θ , a set of m material parameters $\boldsymbol{\kappa} \in \mathbb{R}^m$, etc. There exist a great variety of constitutive relations in the literature according to the above skeletal structure (11) (see e.g. [1, 2] and references herein and [20] concerning fundamental aspects of viscoplasticity). Many approaches intend to provide for a number of different characteristic effects such as strain rate dependent plastic flow, creep or stress relaxation. In doing so, a yield criterion with the inherent specification of loading and unloading conditions is not needed. The resulting equations are currently referred to as

unified models [2]. Concerning the internal variables, in principal they are argued for macroscopic or microscopic reasons depending on the basic conception.

A specific example for a material law of the above type (11) is the following power law with isotropic hardening, which basically is an extension of the well-known Norton law (see e.g. [1, 18]).

$$\left. \begin{aligned} \dot{\boldsymbol{\epsilon}}^{\text{in}} &= \frac{3}{2} \dot{\boldsymbol{\epsilon}} \mathbf{n} \\ \dot{\boldsymbol{\epsilon}} &= \begin{cases} \left(\frac{\Phi(\boldsymbol{\sigma}, R)}{K'} \right)^{n'} & , \text{ if } \Phi(\boldsymbol{\sigma}, R) > 0 \\ 0, & \text{ else} \end{cases} \end{aligned} \right\} \quad (12)$$

Here, \mathbf{n} and Φ are defined in Eq. (8), and $R = \hat{R}(e)$ is given by Eq. (8)₃ or Eq. (10) for the case of exponential or linear hardening, respectively. It can be seen, that, analogously to Eq. (3) for problems in plasticity, a pure elastic domain is introduced. However, as a major difference, the stress state can be such that $\Phi(\boldsymbol{\sigma}, R) > 0$, so that $\Phi(\boldsymbol{\sigma}, R)$ plays the role of an overstress. Furthermore, the model has $m = 5$ material parameters $\boldsymbol{\kappa} = [\sigma_0, n', K', b, q]^T$ for the exponential hardening type and $m = 4$ material parameters $\boldsymbol{\kappa} = [\sigma_0, n', K', H]^T$ for the linear hardening type, which characterize the inelastic material behaviour. In [19] it is shown that the above model can also be interpreted as a penalty regularization of the rate independent model (8).

Lastly, let us note that in view of identification of the material parameters based on experimental investigations, it is useful to distinguish between *observable* and *non-observable* variables (see [1]). In this respect the displacements \mathbf{u} on the surface $\partial\Omega$ are observable variables (and so are the total strains $\boldsymbol{\epsilon}$), whilst, e.g. e and $\boldsymbol{\epsilon}^{\text{in}}$ in (12) are non-observable variables.

2.3. The direct problem

In order to formulate the direct problem as an initial-boundary value problem for the displacements, we summarize the conditions for equilibrium and the boundary and initial conditions, respectively, as

$$\begin{aligned} \text{div} \boldsymbol{\sigma}(\mathbf{u}) - \rho \hat{\mathbf{b}} &= \mathbf{0} && \text{in } \Omega \\ \mathbf{u} &= \hat{\mathbf{u}} && \text{on } \partial\Omega_u \\ \mathbf{t} &= \hat{\mathbf{t}} && \text{on } \partial\Omega_\sigma \\ \mathbf{u}(t=0) &= \mathbf{u}_0, & \mathbf{q}(t=0) &= \mathbf{q}_0, & \boldsymbol{\sigma}(t=0) &= \boldsymbol{\sigma}_0. \end{aligned} \quad (13)$$

Then, assuming given material parameters $\boldsymbol{\kappa} \in \mathbb{R}^m$ along with the constitutive equations of Sections 2.1 or 2.2, respectively, this characterizes the direct problem for the displacements as

$$\boxed{\boldsymbol{\kappa} \mapsto \mathbf{u}(\bullet, \bullet; \boldsymbol{\kappa})} \quad (14)$$

2.4. The inverse problem

Let \bar{U} denote the observation space and let $\bar{\mathbf{u}} \in \bar{U}$ denote given data obtained from experiment. Since in general only incomplete data are available from the experiment, we introduce an observation operator $\mathcal{M}: U \rightarrow \bar{U}$ mapping the displacement trajectory $\mathbf{u}(\bullet, \bullet; \boldsymbol{\kappa})$ to points of the observation space \bar{U} [3]. Then, the inverse problem of (14) is written as

$$\boxed{\text{Find } \boldsymbol{\kappa} : \mathcal{M} \mathbf{u}(\bullet, \bullet; \boldsymbol{\kappa}) = \bar{\mathbf{u}} \text{ for given } \bar{\mathbf{u}} \in \bar{U}.} \quad (15)$$

It is well known that the above problem is ill-posed in the sense of Hadamard [22], and therefore an *optimal approach strategy* is considered to tackle the above problem. To this end the following optimization problem with functional of least-squares type is formulated:

$$f(\boldsymbol{\kappa}) = \frac{1}{2} \|\mathcal{M}\mathbf{u}(\bullet, \bullet; \boldsymbol{\kappa}) - \bar{\mathbf{u}}\|_{\tilde{U}}^2 \longrightarrow \min_{\boldsymbol{\kappa}} \quad (16)$$

REMARKS

- (1) Let $\{\mathbf{x}_i\}_{i=1}^{n_{mp}} \subset \Omega$ be the set of n_{mp} points, where experimental data are available for $\bar{\mathbf{u}}(\mathbf{x}_i, t_j) \in \mathbb{R}^{n_{dim}}$ at $n_{t_{dat}}$ time steps $\{t_j\}_{j=1}^{n_{t_{dat}}}$. Consequently, in this case, the total number of experimental data is $n_{dat} = n_{mp}n_{dim}n_{t_{dat}}$, and we have $\tilde{U} = \mathbb{R}^{n_{dat}}$. Furthermore, the observation operator \mathcal{M} is defined by

$$\mathcal{M}\mathbf{u}(\bullet, \bullet; \boldsymbol{\kappa}) := \{u_1(\mathbf{x}_i, t_j; \boldsymbol{\kappa}), \dots, u_{n_{dim}}(\mathbf{x}_i, t_j; \boldsymbol{\kappa}); i = 1, \dots, n_{mp}, j = 1, \dots, n_{t_{dat}}\} \quad (17)$$

Next, using the definitions

$$\begin{aligned} \mathbf{u}_j(\boldsymbol{\kappa}) &:= \{u_1(\mathbf{x}_i, t_j; \boldsymbol{\kappa}), \dots, u_{n_{dim}}(\mathbf{x}_i, t_j; \boldsymbol{\kappa}); i = 1, \dots, n_{mp}\}, \quad j = 1, \dots, n_{t_{dat}} \\ \mathbf{u}(\boldsymbol{\kappa}) &:= \{\mathbf{u}_j(\boldsymbol{\kappa}), \quad j = 1, \dots, n_{t_{dat}}\} \end{aligned} \quad (18)$$

for the simulated data and analogous expressions for the experimental data $\bar{\mathbf{u}}_j, j = 1, \dots, n_{t_{dat}}$ and $\bar{\mathbf{u}}$, respectively, we can write the least-squares problem (16) as

$$f(\boldsymbol{\kappa}) = \frac{1}{2} \sum_{j=1}^{n_{t_{dat}}} (\mathbf{u}_j(\boldsymbol{\kappa}) - \bar{\mathbf{u}}_j)^T (\mathbf{u}_j(\boldsymbol{\kappa}) - \bar{\mathbf{u}}_j) = \frac{1}{2} \|\mathbf{u}(\boldsymbol{\kappa}) - \bar{\mathbf{u}}\|_2^2 \longrightarrow \min_{\boldsymbol{\kappa}} \quad (19)$$

- (2) In many situations, the problem (19), though well posed, may lead to numerically *unstable solutions*, i.e. small variations of $\bar{\mathbf{u}}$ may lead to large variations of the parameters $\boldsymbol{\kappa}$. These difficulties are caused, e.g. if the material model has (to many) parameters, which are (almost) linearly dependent, or if the experiment is inadequate in the sense that some parameters are not ‘activated’ [8]. E.g. considering a model which is intended for cyclic loading as proposed in [1, 18], the above-mentioned difficulties arise, if only monotonic loading is performed during the experiment instead of cyclic loading [8].

A mathematical tool, suitable to overcome the above-mentioned numerical instabilities is a regularization of the functional in (19), and this leads to the more general problem

$$f(\boldsymbol{\kappa}) = \frac{1}{2} \|\mathbf{B}_\delta (\mathbf{u}(\boldsymbol{\kappa}) - \bar{\mathbf{u}})\|_2^2 + \frac{\alpha}{2} \|\mathbf{B}_\mu (\boldsymbol{\kappa} - \bar{\boldsymbol{\kappa}})\|_2^2 \longrightarrow \min_{\boldsymbol{\kappa}} \quad (20)$$

Here, the matrices $\mathbf{B}_\delta \in \mathbb{R}^{n_{dat}} \times \mathbb{R}^{n_{dat}}$ and $\mathbf{B}_\mu \in \mathbb{R}^m \times \mathbb{R}^m$, the scalar $\alpha \in \mathbb{R}^+$ and the a priori parameters $\bar{\boldsymbol{\kappa}} \in \mathbb{R}^m$ are *regularization parameters*, which can be chosen based on, e.g. a priori information or statistical investigations (see e.g. [23–26] for further discussions and [7, 8] for numerical examples in the context of identification for viscoplastic material models). However, a systematic concept for determination of the regularization parameters in the context of parameter identification so far is not available.

- (3) Let us comment on two different type of errors: For this purpose let \mathbf{u}^* denote the *true state*. Then, even for a correct parameter $\boldsymbol{\kappa}^*$ the following situations may arise [3]

- $\mathcal{M}\mathbf{u}^*(\bullet, \bullet) \neq \bar{\mathbf{u}}$ due *measurement errors*.
- $\mathbf{u}^*(\bullet, \bullet) \neq \mathbf{u}(\bullet, \bullet; \boldsymbol{\kappa}^*)$ due to *model errors*.

The first type of error can be addressed by statistical investigations. In this respect, when considering the maximum Likelihood method, on the basis of sufficient experimental results a normal distribution with known variances leads to the first part of the weighted least-squares function (20) with the weights \mathbf{B}_δ given by the elements of the inverse of covariances (see [23, p. 63]).

The second type of error mentioned above, e.g. is addressed by increasing the complexity of the model, thus decreasing the model error. In doing so, it should be realized, that the introduction of additional material parameters may also result into the aforementioned numerical instability for the identification process, if appropriate steps are not performed when planing the experiment. To summarize, the requirements for numerically *stable results* and *reducing the model error* have to be carefully balanced.

- (4) The above presentation is based on load controlled experiments, where data are available only for the displacements. Of course, analogous arguments hold for experiments, where experimental data are available for the strains. If (complementary) displacement controlled experiments are performed, data are available for forces. Furthermore, a combination of these experimental data may also be used with adequate weighing factors \mathbf{B}_δ .

3. Numerical solution of the direct problem

3.1. Global iteration procedure

We consider a discretization of Ω into n_{elm} non-overlapping finite elements and the discretization of \mathcal{I} into N time intervals according to

$$\Omega_h = \bigcup_{e=1}^{n_{\text{elm}}} \Omega_e, \quad \mathcal{I} = \bigcup_{k=1}^N [t_{k-1}, t_k]. \tag{21}$$

Let n_{dof} denote the dimension for the discrete (global) vector \mathbf{V}_k of (nodal displacement) unknowns at each time step $k = 1, \dots, N$. Then, using vector notation, typically, standard finite element discretization results into the following non-linear system of equations:

$$\mathbf{R}_k = \hat{\mathbf{R}}_k(\mathbf{V}_k) = \mathbf{A} \int_{\Omega_e} \mathbf{B}_e^T \hat{\boldsymbol{\sigma}}_k(\mathbf{V}_k) \, d\Omega_e - \mathbf{R}_{\text{ext}}. \tag{22}$$

Here, $\mathbf{R}_k \in \mathbb{R}^{n_{\text{dof}}}$ is the residual vector, which consists of an internal and an external force vector. Concerning the inner force vector, \mathbf{A} denotes the standard assembly operator, \mathbf{B}_e is the discrete strain matrix and $\hat{\boldsymbol{\sigma}}_k(\mathbf{V}_k)$ is the stress vector.

Furthermore, constitutive equations at each quadrature point have to be satisfied as discussed in the next section, thus yielding the stresses $\boldsymbol{\sigma}_k = \hat{\boldsymbol{\sigma}}_k(\mathbf{V}_k)$ and internal variables $\mathbf{q}_k = \hat{\mathbf{q}}_k(\mathbf{V}_k)$ at each time step for each quadrature point. In this regard displacements are *independent variables*, whilst the stresses and internal variables are *dependent variables*. This implies a solution strategy, where an outer loop, the global iteration procedure iterates for Eq. (22), whilst inner loops (local iterations) iterate for the equations at each quadrature point in a *strain driven algorithm*.

When using a Newton method, solution of the above system of equations (22) is obtained according to

$$\mathbf{V}_k^{(j+1)} = \mathbf{V}_k^{(j)} - \alpha^{(j)} [\mathbf{K}_T^{(j)}]^{-1} \mathbf{R}_k^{(j)}, \tag{23}$$

where the Jacobian of the residual vector

$$\mathbf{K}_T = \frac{d\mathbf{R}_k}{d\mathbf{V}_k} = \mathbf{A} \int_{\Omega_e} \mathbf{B}_e^T \frac{d\boldsymbol{\sigma}_k}{d\boldsymbol{\varepsilon}_k} \mathbf{B}_e \, d\Omega_e \tag{24}$$

is known as the consistent tangent matrix [27]. The determination of the global tangent matrix $\mathbf{C}_T = d\boldsymbol{\sigma}_k/d\boldsymbol{\varepsilon}_k$ shall be considered in Section 3.3.

REMARKS

- (1) The line search parameter (or damping parameter) in $\alpha^{(j)}$ Eq. (23) is a necessary tool for attaining global convergence of the algorithm in the case of improper starting vectors $\mathbf{V}_k^{(j=0)}$. In our numerical tests $\alpha^{(j)}$ is determined with an Armijo like line search, where

$$F(\mathbf{V}_k) := \|\hat{\mathbf{R}}_k(\mathbf{V}_k)\| \tag{25}$$

serves as a merit function (see [28, p. 147]).

- (2) As noted in [29] the *assumed strain method* described by Simo/Rifai is applied in the same manner as standard finite element displacements methods. Here, a set of so-called strain variables α_k is added to the independent variables \mathbf{V}_k (see [29] for further details). Note that, when applying line search computations, the condensed residual vector is not suitable to define the merit function (25). Instead, it becomes necessary to use the residual of the uncondensed system of equations.
- (3) Note, that a factorization (Gauss or Cholesky) of \mathbf{K}_T in Eq. (23) can be avoided for large scaled systems, when using a Newton multigrid method as proposed in [30].

3.2. Local iteration procedure

The basic problem of a *strain driven* algorithm at the quadrature point level is as follows: It is the object to find stresses and internal variables $\{\boldsymbol{\sigma}_k, \mathbf{q}_k\}$ at time t_k for given initial values $\{\boldsymbol{\sigma}_{k-1}, \mathbf{q}_{k-1}\}$ and given total strain $\boldsymbol{\varepsilon}_k$ at each quadrature point $\mathbf{x}_{ig} \in \Omega^h$, $ig = 1, Ng$, as discussed below. It is noteworthy that the basic problem in the context of assumed strain methods is the same as for standard finite displacement methods (see [29] for further details).

Concerning the following notation, we will not explicitly distinguish between tensorial or vectorial notation for the stresses $\boldsymbol{\sigma}$. Frequently, we will adopt the term modulus, where depending on the context in tensor notation this quantity is a fourth-order tensor $\mathcal{S} \rightarrow \mathcal{S}$, whilst in vector notation we have a matrix $\mathbb{R}^{n_{\text{str}}} \rightarrow \mathbb{R}^{n_{\text{str}}}$, where n_{str} is the dimension for the stress vector depending on the problem at hand.

3.2.1. Formulation of the discretized problem

The starting point of our discussion for problems of visco-plasticity are the equations (2), (7) and (11), respectively. Combining these equations the discrete analogue equations at each time step $k = 1, \dots, N$ read

$$\begin{aligned} \boldsymbol{\sigma}_k &= \mathbf{C}\boldsymbol{\varepsilon}_k - \mathbf{C}(\boldsymbol{\varepsilon}_{k-1}^{\text{in}} + \Delta\boldsymbol{\varepsilon}_k^{\text{in}}) \\ \mathbf{q}_k &= \mathbf{q}_{k-1} + \Delta\mathbf{q}_k, \end{aligned} \tag{26}$$

where, e.g. by use of a generalized midpoint rule we have the relations

$$\begin{aligned} \Delta\boldsymbol{\varepsilon}_k^{\text{in}} &= \Delta t_k \dot{\boldsymbol{\varepsilon}}^{\text{in}}((1 - \alpha)\boldsymbol{\sigma}_k + \alpha\boldsymbol{\sigma}_{k-1}, (1 - \alpha)\mathbf{q}_k + \alpha\mathbf{q}_{k-1}, \dots; \boldsymbol{\kappa}) \\ \Delta\mathbf{q}_k &= \Delta t_k \dot{\mathbf{q}}((1 - \alpha)\boldsymbol{\sigma}_k + \alpha\boldsymbol{\sigma}_{k-1}, (1 - \alpha)\mathbf{q}_k + \alpha\mathbf{q}_{k-1}, \dots; \boldsymbol{\kappa}), \end{aligned} \tag{27}$$

and where $\Delta t_k = t_k - t_{k-1}$ is the time step. Next, from Eq. (26) the following non-linear system of equations is reformulated:

$$\mathbf{G}_k = \hat{\mathbf{G}}_k(\mathbf{Y}_k) := \begin{bmatrix} \mathbf{g}_{1,k} \\ \mathbf{g}_{2,k} \end{bmatrix} = \mathbf{0}, \tag{28}$$

where

$$\begin{aligned} \mathbf{Y}_k &:= [\boldsymbol{\sigma}_k, \mathbf{q}_k] \\ \mathbf{g}_{1,k} &:= \boldsymbol{\sigma}_k - \boldsymbol{\sigma}_{k-1} - \mathbf{C}(\boldsymbol{\varepsilon}_k - \boldsymbol{\varepsilon}_{k-1}) + \mathbf{C}\Delta\boldsymbol{\varepsilon}_k^{\text{in}} \\ \mathbf{g}_{2,k} &:= \mathbf{q}_k - \mathbf{q}_{k-1} - \Delta\mathbf{q}_k \end{aligned} \tag{29}$$

Frequently, we shall denote \mathbf{G}_k as the *local state equation*, and \mathbf{Y}_k contains the *state variables* $\boldsymbol{\sigma}_k$ and \mathbf{q}_k . Referring to vector notation for 3-D problems we define $\mathbf{Y}_k^{3\text{-D}} := [\sigma_x, \sigma_y, \sigma_z, \tau_{xy}, \tau_{yz}, \tau_{xz}, \mathbf{q}]_k^T$, and for plane strain problems we have $\mathbf{Y}_k^{P\text{Strn}} := [\sigma_x, \sigma_y, \tau_{xy}, \sigma_z, \mathbf{q}]_k^T$.

EXAMPLES

- (1) We consider the power law (12) with an Euler-backward scheme, i.e. $\alpha = 0$ in Eq. (27). Furthermore, we assume $\Phi(\boldsymbol{\sigma}_k^T, \hat{R}(e_{k-1})) > 0$, so that viscoplastic loading takes place, where $\boldsymbol{\sigma}_k^T := \boldsymbol{\sigma}_{k-1} + \mathbf{C}(\boldsymbol{\varepsilon}_k - \boldsymbol{\varepsilon}_{k-1})$ is the elastic predictor. Then, the discrete equations read

$$\begin{aligned} \mathbf{Y}_k &:= [\boldsymbol{\sigma}_k, e_k] \\ \mathbf{g}_{1,k} &:= \boldsymbol{\sigma}_k - \boldsymbol{\sigma}_{k-1} - \mathbf{C}(\boldsymbol{\varepsilon}_k - \boldsymbol{\varepsilon}_{k-1}) + 3\mu(e_k - e_{k-1}) \mathbf{n}_k \\ \mathbf{g}_{2,k} &:= e_k - e_{k-1} + \left(\frac{\Phi(\boldsymbol{\sigma}_k, \hat{R}(e_k))}{K'} \right)^{n'} \Delta t_k \end{aligned} \quad (30)$$

where $\Phi(\boldsymbol{\sigma}_k, e_k) = \sigma_v(\boldsymbol{\sigma}) - (\sigma_0 + \hat{R}(e_k))$ and where $\hat{R}(e_k)$ is specified in Eqs. (8)₃ or (10), respectively.

- (2) For problems of plasticity we assume $\Phi(\boldsymbol{\sigma}_k^T, e_{k-1}) > 0$ for the elastic predictor, so that plastic loading takes place. Then, the yield criterion is added to the state equation (28), and the inelastic strain e_k is viewed as an additional component of the vector of state variables \mathbf{Y}_k . Consequently, using the relation $\lambda_k = e_k - e_{k-1}$ (which eliminates the analogous equation of (30)₃), by use of an Euler-backward rule for the case of single surface plasticity we have

$$\begin{aligned} \mathbf{Y}_k &:= [\boldsymbol{\sigma}_k, e_k] \\ \mathbf{g}_{1,k} &:= \boldsymbol{\sigma}_k - \boldsymbol{\sigma}_{k-1} - \mathbf{C}(\boldsymbol{\varepsilon}_k - \boldsymbol{\varepsilon}_{k-1}) + 3\mu(e_k - e_{k-1}) \mathbf{n}_k \\ \mathbf{g}_{2,k} &:= \Phi(\boldsymbol{\sigma}_k, e_k) = \sigma_v(\boldsymbol{\sigma}) - (\sigma_0 + \hat{R}(e_k)) \end{aligned} \quad (31)$$

Here, as before, $\hat{R}(e_k)$ is specified in Eqs. (8)₃ or (10), respectively.

3.2.2. Local tangent moduli

For solution of the above examples (30) and (31) very efficient algorithms exist in the literature, by reducing the problem to a scalar equation, which is solved by a Newton iteration procedure. The resulting algorithm is referred to as Radial Return method firstly proposed by Wilkens [31] and Krieg and Key [32] (see also [19] for further details).

However, in some situations with complex material laws the above-mentioned reduction is not possible. In e.g. [33] it is shown, that when integrating problems of plasticity with additional non-linear kinematic hardening both the plastic multiplier *and* stress-like variables have to be chosen as unknowns for an extended non-linear system of equations (see [33] for more details). Motivated by this example we present in a systematic manner an algorithm for the local iteration procedure, flexible enough to account for a general yield condition, flow rule and hardening law. In the forthcoming sections it will also be shown that extension to plane stress problems becomes very simple. Furthermore, we will exploit the structure of so-called local tangent moduli derived in this section in order to obtain the tangent matrix of the global iteration procedure in the next section and in order to perform the sensitivity analysis for the corresponding inverse problem in Section 4.3.

The aim of the local iteration is to determine the state variables \mathbf{Y}_k such that Eq. (28) is satisfied within some tolerance. By use of a damped Newton method the iteration scheme is defined as

$$\mathbf{Y}_k^{(j+1)} = \mathbf{Y}_k^{(j)} + \alpha^{(j)} \Delta \mathbf{Y}_k^{(j)} \quad (32)$$

Here, $\Delta \mathbf{Y}_k = [\Delta \boldsymbol{\sigma}_k, \Delta q_k]$ is obtained from solution of the linear system of equations

$$\mathbf{J}_k^{(j)} \Delta \mathbf{Y}_k^{(j)} = \mathbf{G}^{(j)} \quad (33)$$

and

$$\mathbf{J}_k^{(j)} := \left. \frac{\partial \mathbf{G}_k}{\partial \mathbf{Y}_k} \right|_{\mathbf{Y}_k = \mathbf{Y}_k^{(j)}} \tag{34}$$

is the Jacobian of $\mathbf{G}_k(\mathbf{Y}_k)$ at $\mathbf{Y}_k = \mathbf{Y}_k^{(j)}$. The above linear system of equations may be solved directly with a Gaussian method.

Alternatively, a standard condensation procedure can be applied as follows: To this end (and suppressing the upper index in $(\bullet)^{(j)}$) we consider the following partition of Eq. (33)

$$\begin{bmatrix} \frac{\partial \mathbf{g}_{1,k}}{\partial \boldsymbol{\sigma}_k} & \frac{\partial \mathbf{g}_{1,k}}{\partial \mathbf{q}_k} \\ \frac{\partial \mathbf{g}_{2,k}}{\partial \boldsymbol{\sigma}_k} & \frac{\partial \mathbf{g}_{2,k}}{\partial \mathbf{q}_k} \end{bmatrix} \begin{bmatrix} \Delta \boldsymbol{\sigma}_k \\ \Delta \mathbf{q}_k \end{bmatrix} = \begin{bmatrix} \mathbf{g}_{1,k} \\ \mathbf{g}_{2,k} \end{bmatrix}. \tag{35}$$

Then, according to Lemma 1 of Appendix, A, the solution of the above linear systems of equations can be obtained from:

$$\begin{cases} \Delta \boldsymbol{\sigma}_k = \tilde{\mathbf{C}}_\sigma \tilde{\mathbf{g}}_{1,k} \\ \Delta \mathbf{q}_k = \tilde{\mathbf{C}}_q \tilde{\mathbf{g}}_{2,k} \end{cases}, \tag{36}$$

where

$$\begin{cases} \tilde{\mathbf{C}}_\sigma = \left[\frac{\partial \mathbf{g}_{1,k}}{\partial \boldsymbol{\sigma}_k} - \frac{\partial \mathbf{g}_{1,k}}{\partial \mathbf{q}_k} \left[\frac{\partial \mathbf{g}_{2,k}}{\partial \mathbf{q}_k} \right]^{-1} \frac{\partial \mathbf{g}_{2,k}}{\partial \boldsymbol{\sigma}_k} \right]^{-1} \\ \tilde{\mathbf{C}}_q = \left[\frac{\partial \mathbf{g}_{2,k}}{\partial \mathbf{q}_k} \right]^{-1} \\ \tilde{\mathbf{g}}_{1,k} = \mathbf{g}_{1,k} - \frac{\partial \mathbf{g}_{1,k}}{\partial \mathbf{q}_k} \left[\frac{\partial \mathbf{g}_{2,k}}{\partial \mathbf{q}_k} \right]^{-1} \mathbf{g}_{2,k} \\ \tilde{\mathbf{g}}_{2,k} = \mathbf{g}_{2,k} - \frac{\partial \mathbf{g}_{2,k}}{\partial \boldsymbol{\sigma}_k} \Delta \boldsymbol{\sigma}_k \end{cases} \tag{37}$$

In the sequel of this work we shall denote $\tilde{\mathbf{C}}_\sigma$ and $\tilde{\mathbf{C}}_q$ as *local tangent moduli* for the stresses and the internal variables, respectively. From the above equations it can be seen, that at least *partial derivatives* of the state equations $\mathbf{g}_{1,k}$ and $\mathbf{g}_{2,k}$ are required for its determination. The evaluation of (36) can also be performed directly by use of a Gaussian factorization. Alternatively, in many cases it is possible to proceed analytically. Then, *explicit formulas* for its representation are obtained. In Appendix B we will specify this issue for the case of J_2 -flow theory.

Let us mention again that the above iteration scheme (32)–(34) is not recommended for material laws with a simple structure as, e.g. in J_2 -flow theory, where standard radial return methods are more efficient. However, the above representation gives some prerequisite insight into the results that follow below.

3.3. Global tangent modulus

As mentioned before, the (consistent) global tangent modulus is defined as

$$\mathbf{C}_T := \frac{d\boldsymbol{\sigma}_k}{d\boldsymbol{\varepsilon}_k} \tag{38}$$

at the converged state of the local iteration procedure. A unified expression for \mathbf{C}_T based on the formulation of Section 3.2.2 can now be obtained as the following result shows:

PROPOSITION 1: Let $\tilde{\mathbf{C}}_\sigma$ and \mathbf{C} be the local tangent modulus for the stresses (37)₁ and the elasticity modulus obtained from (5)₂, respectively. Then, the (consistent) global tangent modulus is given by

$$\boxed{\mathbf{C}_T = \tilde{\mathbf{C}}_\sigma \mathbf{C}} \tag{39}$$

PROOF. We recall that a standard iteration scheme for solution of the non-linear systems of equations is regarded as a strain driven algorithm. In this respect, the state variables $\boldsymbol{\sigma}_k, \mathbf{q}_k$ are dependent on $\boldsymbol{\varepsilon}_k$. Therefore, the state equation (28) (at the converged state of the local iteration procedure) may be seen as a function dependent on $\boldsymbol{\varepsilon}_k$, both explicitly and implicitly:

$$\mathbf{G}_k = \hat{\mathbf{G}}_k(\boldsymbol{\varepsilon}_k, \boldsymbol{\sigma}_k(\boldsymbol{\varepsilon}_k), \mathbf{q}_k(\boldsymbol{\varepsilon}_k)) = \mathbf{0}. \tag{40}$$

Next, we consider the total differential

$$\frac{d\mathbf{G}_k}{d\boldsymbol{\varepsilon}_k} = \frac{\partial \mathbf{G}_k}{\partial \boldsymbol{\varepsilon}_k} + \frac{\partial \mathbf{G}_k}{\partial \boldsymbol{\sigma}_k} \frac{d\boldsymbol{\sigma}_k}{d\boldsymbol{\varepsilon}_k} + \frac{\partial \mathbf{G}_k}{\partial \mathbf{q}_k} \frac{d\mathbf{q}_k}{d\boldsymbol{\varepsilon}_k} = \mathbf{0}, \tag{41}$$

and with the partition of Eq. (35) we write

$$\begin{aligned} \frac{d\mathbf{g}_{1,k}}{d\boldsymbol{\varepsilon}_k} &= \frac{\partial \mathbf{g}_{1,k}}{\partial \boldsymbol{\sigma}_k} \frac{d\boldsymbol{\sigma}_k}{d\boldsymbol{\varepsilon}_k} + \frac{\partial \mathbf{g}_{1,k}}{\partial \mathbf{q}_k} \frac{d\mathbf{q}_k}{d\boldsymbol{\varepsilon}_k} + \frac{\partial \mathbf{g}_{1,k}}{\partial \boldsymbol{\varepsilon}_k} = \mathbf{0} \\ \frac{d\mathbf{g}_{2,k}}{d\boldsymbol{\varepsilon}_k} &= \frac{\partial \mathbf{g}_{2,k}}{\partial \boldsymbol{\sigma}_k} \frac{d\boldsymbol{\sigma}_k}{d\boldsymbol{\varepsilon}_k} + \frac{\partial \mathbf{g}_{2,k}}{\partial \mathbf{q}_k} \frac{d\mathbf{q}_k}{d\boldsymbol{\varepsilon}_k} = \mathbf{0}. \end{aligned} \tag{42}$$

In the above equation (42)₂ we used the fact, that $\mathbf{g}_{2,k}$ is *not* dependent on $\boldsymbol{\varepsilon}_k$. Next, solving Eq. (42)₂ for $d\mathbf{q}_k/d\boldsymbol{\varepsilon}_k$, and substituting into (42)₁ entails writing

$$\frac{d\boldsymbol{\sigma}_k}{d\boldsymbol{\varepsilon}_k} = - \left[\frac{\partial \mathbf{g}_{1,k}}{\partial \boldsymbol{\sigma}_k} - \frac{\partial \mathbf{g}_{1,k}}{\partial \mathbf{q}_k} \left[\frac{\partial \mathbf{g}_{2,k}}{\partial \mathbf{q}_k} \right]^{-1} \frac{\partial \mathbf{g}_{2,k}}{\partial \boldsymbol{\sigma}_k} \right]^{-1} \frac{\partial \mathbf{g}_{1,k}}{\partial \boldsymbol{\varepsilon}_k}. \tag{43}$$

Comparing the result with Eq. (37)₁, the local tangent modulus for the stresses, and noting that $-\partial \mathbf{g}_{1,k}/\partial \boldsymbol{\varepsilon}_k = \mathbf{C}$, the elasticity modulus the result (39) follows. \square

Thus, having provided the local tangent modulus $\tilde{\mathbf{C}}_\sigma$ —with a direct factorization strategy or analytically—the global tangent modulus is easily obtained by the above product (39). In Appendix B we will consider this issue in more detail for J_2 -flow theory.

3.4. Extension to plane stress problems

As noted in [35], a simple radial return in plasticity would violate the plane stress condition. Of course, the same implication holds for our iteration procedure described in Section 3.2.2. However, the algorithm discussed above can be easily extended to plane stress problems as follows:

Using vector notation, the central idea consists in defining the vector of state variables as

$$\mathbf{Y}_k^{PStns} := [\sigma_x, \sigma_y, \tau_{xy}, \varepsilon_z, \mathbf{q}]_k, \tag{44}$$

i.e. contrary to 3-D or plane strain problems the strain $\varepsilon_{z,k}$ is viewed as an unknown for the non-linear system of equations $\mathbf{G}_k(\mathbf{Y}_k)$.

Next, we define

$$\mathbf{C}_\sigma^{PStrn} := \left[\frac{\partial \mathbf{g}_{1,k}}{\partial \boldsymbol{\sigma}_k} - \frac{\partial \mathbf{g}_{1,k}}{\partial \mathbf{q}_k} \left[\frac{\partial \mathbf{g}_{2,k}}{\partial \mathbf{q}_k} \right]^{-1} \frac{\partial \mathbf{g}_{2,k}}{\partial \boldsymbol{\sigma}_k} \right] \tag{45}$$

as the inverse of $\tilde{\mathbf{C}}_\sigma^{PStrn}$ in Eq. (37)₁. Then, straightforward manipulation shows, that the local tangent matrix for plane stress problems is given by

$$\begin{aligned} \tilde{\mathbf{C}}_\sigma^{PStrs} &= [\mathbf{C}_\sigma^{PStrn} + (\mathbf{b} - \mathbf{c}) \otimes \mathbf{1}^+]^{-1} \\ \mathbf{b} &:= [-\lambda, -\lambda, 0, -2\mu - \lambda]^T \\ (\mathbf{c})_i &:= (\mathbf{C}_\sigma^{PStrn})_{i,j=4}, \quad i = 1, \dots, 4 \\ \mathbf{1}^+ &:= [0, 0, 0, 1]^T, \end{aligned} \tag{46}$$

where μ and λ are the Lamé constants. Concerning the global consistent matrix let us assume the following partition of $\tilde{\mathbf{C}}_\sigma^{PStrs}$ and the elasticity matrix \mathbf{C} , respectively

$$\tilde{\mathbf{C}}_\sigma^{PStrs} = \begin{bmatrix} \mathbf{A}_\sigma & \mathbf{b}_\sigma \\ \mathbf{c}_\sigma^T & d_\sigma \end{bmatrix}, \quad \mathbf{C} = \begin{bmatrix} \mathbf{A}_C & \mathbf{b}_C \\ \mathbf{c}_C^T & d_C \end{bmatrix}, \tag{47}$$

where $\mathbf{A}_\sigma, \mathbf{A}_C \in \mathbb{R}^3 \otimes \mathbb{R}^3$, $\mathbf{b}_\sigma, \mathbf{b}_C, \mathbf{c}_\sigma, \mathbf{c}_C \in \mathbb{R}^3$, and $d_\sigma, d_C \in \mathbb{R}$. Then, the 3×3 consistent global matrix is obtained from

$$\mathbf{C}_T^{PStrs} = \left(\mathbf{A}_\sigma - \frac{1}{d_\sigma} \mathbf{b}_\sigma \otimes \mathbf{c}_\sigma \right) \left(\mathbf{A}_C - \frac{1}{d_C} \mathbf{b}_C \otimes \mathbf{c}_C \right). \tag{48}$$

4. Numerical solution of the inverse problem

4.1. Formulation of the problem

As before, let $\bar{\mathbf{u}}_j = \{\bar{u}_1(\mathbf{x}_i, t_j), \dots, \bar{u}_{n_{dim}}(\mathbf{x}_i, t_j); i = 1, \dots, n_{mp}\}$ denote the $n_{mp}n_{dim}$ experimental data at each time step t_j , $j = 1, \dots, n_{dat}$. Furthermore, for ease of explanation we assume that the sets of time steps for integration $\{t_k\}_{k=1}^N$ and for the experimental data $\{t_j\}_{j=1}^{n_{dat}}$ do coincide. The following considerations can be extended to more complex situations in a straightforward manner. Next, we introduce a discrete observation operator $\bar{\mathcal{M}}: \mathbb{R}^{n_{dof}} \rightarrow \mathbb{R}^{n_{dat}}$, which maps the set of displacements \mathbf{V}_k to the vector space of experimental data at each time step t_k , $k = 1, \dots, N$. (It is noteworthy, that in a more general setting $\bar{\mathcal{M}}$ would not be constant for all time steps.) With this notation at hand and noting that additionally the global state equation (22) has to be satisfied for all time steps $k = 1, \dots, N$ the resulting non-linear optimization problem with constraints reads

$$\boxed{\begin{aligned} f(\boldsymbol{\kappa}, \{\mathbf{V}_k\}_{k=1}^N) &= \frac{1}{2} \sum_{k=1}^N (\bar{\mathcal{M}}\mathbf{V}_k - \bar{\mathbf{u}}_k)^T (\bar{\mathcal{M}}\mathbf{V}_k - \bar{\mathbf{u}}_k) \longrightarrow \min_{\boldsymbol{\kappa}, \{\mathbf{V}_k\}_{k=1}^N} \\ \mathbf{R}(\boldsymbol{\kappa}, \mathbf{V}_k) &= \mathbf{0}, \quad k = 1, \dots, N \end{aligned}} \tag{49}$$

It follows, that $\boldsymbol{\kappa}, \{\mathbf{V}_k\}_{k=1}^N$ defines the set of unknowns for the above optimization problem.

4.2. Solution strategy

The following strategy proves to be efficient for solution of the above problem (49): Outer loops are performed which iterate for the material parameters whilst inner loops with a standard finite-element algorithm iterate for solution of the corresponding direct problem. In this regard the material parameters are independent variables whilst the displacements \mathbf{V}_k are dependent variables, i.e. $\mathbf{V}_k = \tilde{\mathbf{V}}_k(\boldsymbol{\kappa})$, $k = 1, \dots, N$ (see [12] for further discussions). Consequently, the optimization problem (49) is replaced by the following problem without constraints

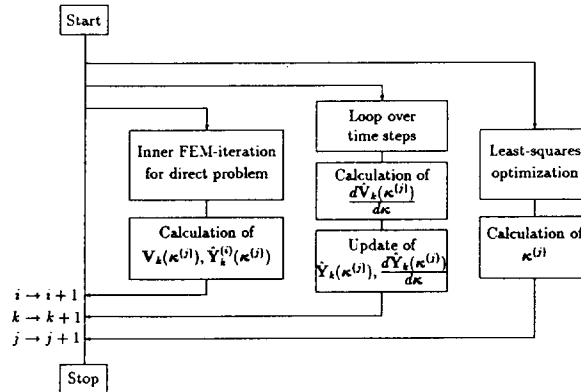


Fig. 1. Schematic flow chart for the identification process with outer and inner iteration loops

$$\begin{aligned}
 f(\boldsymbol{\kappa}) &= \frac{1}{2} \sum_{k=1}^N \left(\bar{\mathcal{M}} \hat{\mathbf{V}}_k(\boldsymbol{\kappa}) - \bar{\mathbf{u}}_k \right)^T \left(\bar{\mathcal{M}} \hat{\mathbf{V}}_k(\boldsymbol{\kappa}) - \bar{\mathbf{u}}_k \right) \longrightarrow \min_{\boldsymbol{\kappa}} \\
 \text{where } \left\{ \hat{\mathbf{V}}_k(\boldsymbol{\kappa}) \right\}_{k=1}^N &\text{ is defined to satisfy} \\
 \mathbf{R}(\boldsymbol{\kappa}, \hat{\mathbf{V}}_k(\boldsymbol{\kappa})) &= \mathbf{0}, \quad k = 1, \dots, N
 \end{aligned}
 \tag{50}$$

A schematic flow chart of the resulting algorithm with a simplified description is shown in Fig. 1. Of course this conception is borrowed from strategies in *shape-optimization*, where in the corresponding terminology the material parameters are the *design variables* of the optimization problem (see e.g. [14,34]).

4.3. Sensitivity analysis

As mentioned before, gradient based methods prove to be much more efficient as methods which use only values of the least-squares functional, and consequently the gradient of the least-squares functional has to be determined. Since the solution strategy described above is similar to procedures in shape optimization, we will adopt the term *sensitivity analysis* for this task.

There exist a large amount of publications in the literature on this topic (for an overview see e.g. [14, 34]). Two different conceptions may be distinguished: [14]: i.e. the *variational sensitivity analysis* and the *discrete sensitivity analysis*. In the first conception, firstly the gradient of the continuous problem with respect to the design variables is determined. The corresponding relations are discretized in space and time consistent with the discretization procedure for the direct problem. The latter conception starts with discretization of the optimization problem at hand, followed by the determination of the gradient of the discretized relations with respect to the design variables.

In this work we will only resort to the second conception, since all discretized relations are at hand in Eq. (50) along with the discretized relations of the previous sections. Then, clearly the gradient for the least-squares functional in (50)₁ is given by

$$\frac{df(\boldsymbol{\kappa})}{d\boldsymbol{\kappa}} = \sum_{k=1}^N \left(\bar{\mathcal{M}} \hat{\mathbf{V}}_k(\boldsymbol{\kappa}) - \bar{\mathbf{u}}_k \right)^T \bar{\mathcal{M}} \frac{d\hat{\mathbf{V}}_k(\boldsymbol{\kappa})}{d\boldsymbol{\kappa}}.
 \tag{51}$$

It follows that essentially the term $d\hat{\mathbf{V}}_k(\boldsymbol{\kappa})/d\boldsymbol{\kappa}$ is needed at each time step $k = 1, \dots, N$. For this reason we consider the implicit function (50)₂—at the converged state of the global iteration procedure—and consequently the total differential is given by

$$\frac{d\mathbf{R}_k}{d\boldsymbol{\kappa}} = \frac{d^p \mathbf{R}_k}{d^p \boldsymbol{\kappa}} + \underbrace{\frac{\partial \mathbf{R}_k}{\partial \mathbf{V}_k}}_{\mathbf{K}_T} \frac{d\mathbf{V}_k}{d\boldsymbol{\kappa}} = \mathbf{0}. \tag{52}$$

Here, the symbol $(\bullet)^p$ for the *partial load vector* $d^p \mathbf{R}_k / d^p \boldsymbol{\kappa}$ is introduced in order to refer to the fact that implicit dependence of $\boldsymbol{\kappa}$ via the displacements $\mathbf{V}_k(\boldsymbol{\kappa})$ is not taken into account.

Solving Eq. (52) for the unknowns yields

$$\frac{d\mathbf{V}_k}{d\boldsymbol{\kappa}} = -[\mathbf{K}_T]^{-1} \frac{d^p \mathbf{R}_k}{d^p \boldsymbol{\kappa}}, \tag{53}$$

where we additionally made use of Eq. (24) for the tangent stiffness matrix \mathbf{K}_T . Note, that in order to solve the above equation, a factorization of \mathbf{K}_T is available from the converged state for solution of the direct problem.

In a geometric linear theory, the partial load vector is obtained from Eq. (22) as

$$\frac{d^p \mathbf{R}_k}{d^p \boldsymbol{\kappa}} = \mathbf{A} \int_{\Omega_e} \mathbf{B}_e^T \frac{d^p \boldsymbol{\sigma}_k}{d^p \boldsymbol{\kappa}} d\Omega_e, \tag{54}$$

and thus it remains to determine the partial derivative $d^p \boldsymbol{\sigma}_k / d^p \boldsymbol{\kappa}$. For problems of elasticity explicit expressions are obtainable for this term, since the stresses are explicitly dependent on the parameters (see [14]). For inelastic problems, however, the state variables $(\boldsymbol{\sigma}_k, \mathbf{q}_k)$ are defined by the state equation (28) (at the converged state of both the local and the global iteration procedure), and thus are dependent on $\boldsymbol{\kappa}$ both explicitly and implicitly [12].

We will show below, that the basic relations needed in the computation of the partial derivative $d^p \boldsymbol{\sigma}_k / d^p \boldsymbol{\kappa}$ are contained in the following result:

PROPOSITION 2: The total derivatives of the state variables $\mathbf{Y}_k = [\boldsymbol{\sigma}_k, \mathbf{q}_k]$ with respect to the material parameters $\boldsymbol{\kappa}$ are given by

$$\begin{aligned} \frac{d\boldsymbol{\sigma}_k}{d\boldsymbol{\kappa}} &= -\tilde{\mathbf{C}}_\sigma \left(\mathbf{h}_{1,k} - \frac{\partial \mathbf{g}_{1,k}}{\partial \mathbf{q}_k} \left[\frac{\partial \mathbf{g}_{2,k}}{\partial \mathbf{q}_k} \right]^{-1} \mathbf{h}_{2,k} \right) \\ \frac{d\mathbf{q}_k}{d\boldsymbol{\kappa}} &= -\tilde{\mathbf{C}}_q \left(\mathbf{h}_{2,k} - \frac{\partial \mathbf{g}_{2,k}}{\partial \boldsymbol{\sigma}_k} \frac{d\boldsymbol{\sigma}_k}{d\boldsymbol{\kappa}} \right) \end{aligned} \tag{55}$$

where

$$\begin{aligned} \mathbf{h}_{1,k} &:= \frac{\partial \mathbf{g}_{1,k}}{\partial \boldsymbol{\kappa}} + \frac{\partial \mathbf{g}_{1,k}}{\partial \mathbf{Y}_{k-1}} \frac{d\mathbf{Y}_{k-1}}{d\boldsymbol{\kappa}} + \frac{\partial \mathbf{g}_{1,k}}{\partial \boldsymbol{\varepsilon}_k} \frac{d\boldsymbol{\varepsilon}_k}{d\boldsymbol{\kappa}} + \frac{\partial \mathbf{g}_{1,k}}{\partial \boldsymbol{\varepsilon}_{k-1}} \frac{d\boldsymbol{\varepsilon}_{k-1}}{d\boldsymbol{\kappa}} \\ \mathbf{h}_{2,k} &:= \frac{\partial \mathbf{g}_{2,k}}{\partial \boldsymbol{\kappa}} + \frac{\partial \mathbf{g}_{2,k}}{\partial \mathbf{Y}_{k-1}} \frac{d\mathbf{Y}_{k-1}}{d\boldsymbol{\kappa}} \end{aligned}, \tag{56}$$

and where the local tangent moduli $\tilde{\mathbf{C}}_\sigma$ and $\tilde{\mathbf{C}}_q$ are defined in Eq. (37).

PROOF. We consider the state equation \mathbf{G}_k as introduced in Eq. (28), however the set of variables is extended by those variables, which depend on the material parameters $\boldsymbol{\kappa}$:

$$\mathbf{G}_k = \hat{\mathbf{G}}_k(\boldsymbol{\kappa}, \hat{\mathbf{Y}}_k(\boldsymbol{\kappa}), \hat{\mathbf{Y}}_{k-1}(\boldsymbol{\kappa}), \hat{\boldsymbol{\varepsilon}}_k(\boldsymbol{\kappa}), \hat{\boldsymbol{\varepsilon}}_{k-1}(\boldsymbol{\kappa})) = \mathbf{0}, \tag{57}$$

where $(\bullet)_k(\boldsymbol{\kappa})$ and $(\bullet)_{k-1}(\boldsymbol{\kappa})$ denote the vectors for the state variables and the total strains at the actual and the previous time step, respectively. The total differential of Eq. (57) is given by

$$\frac{d\mathbf{G}_k}{d\boldsymbol{\kappa}} = \frac{\partial \mathbf{G}_k}{\partial \boldsymbol{\kappa}} + \frac{\partial \mathbf{G}}{\partial \mathbf{Y}_k} \frac{d\mathbf{Y}_k}{d\boldsymbol{\kappa}} + \frac{\partial \mathbf{G}_k}{\partial \mathbf{Y}_{k-1}} \frac{d\mathbf{Y}_{k-1}}{d\boldsymbol{\kappa}} + \frac{\partial \mathbf{G}}{\partial \boldsymbol{\varepsilon}_k} \frac{d\boldsymbol{\varepsilon}_k}{d\boldsymbol{\kappa}} + \frac{\partial \mathbf{G}_k}{\partial \boldsymbol{\varepsilon}_{k-1}} \frac{d\boldsymbol{\varepsilon}_{k-1}}{d\boldsymbol{\kappa}} = \mathbf{0}, \tag{58}$$

and we deduce

$$\frac{d\mathbf{Y}_k}{d\boldsymbol{\kappa}} = - \left[\begin{array}{c} \frac{\partial \mathbf{G}_k}{\partial \mathbf{Y}_k} \\ \frac{\partial \mathbf{Y}_k}{\partial \boldsymbol{\kappa}} \end{array} \right]^{-1} \left(\begin{array}{c} \frac{\partial \mathbf{G}_k}{\partial \boldsymbol{\kappa}} \\ \frac{\partial \mathbf{G}_k}{\partial \mathbf{Y}_{k-1}} \frac{d\mathbf{Y}_{k-1}}{d\boldsymbol{\kappa}} \\ \frac{\partial \mathbf{G}_k}{\partial \boldsymbol{\varepsilon}_k} \frac{d\boldsymbol{\varepsilon}_k}{d\boldsymbol{\kappa}} \\ \frac{\partial \mathbf{G}_k}{\partial \boldsymbol{\varepsilon}_{k-1}} \frac{d\boldsymbol{\varepsilon}_{k-1}}{d\boldsymbol{\kappa}} \end{array} \right). \tag{59}$$

Next, applying Lemma 1 of Appendix A, using the fact that $\mathbf{g}_{2,k}$ is not dependent on $\boldsymbol{\varepsilon}_k$ and using the same condensation procedure as for solution of (33) in Section 3.2.2, the result (55), (56) follows. \square

The result (55), (56) shows that, basically, *partial derivatives* of the state equation \mathbf{G}_k in Eq. (57) with respect to $\boldsymbol{\kappa}, \mathbf{Y}_k, \mathbf{Y}_{k-1}, \boldsymbol{\varepsilon}_k, \boldsymbol{\varepsilon}_{k-1}$ are required. Concerning Terms 1–6 in Eq. (59), which are needed for evaluation of (55) and (56), the following remarks are noteworthy:

Term 1 This term corresponds to the Jacobian \mathbf{J}_k introduced in Eq. (34).

Term 2 For this term the partial derivatives of the state equation \mathbf{G}_k with respect to the material parameters $\boldsymbol{\kappa}$ are required. The result for J_2 -flow theory is presented in Appendix, Part B.

Term 3 Having provided the Jacobian $\mathbf{J}_k = \partial \mathbf{G}_k / \partial \mathbf{Y}_k$, this term usually is easily obtained: E.g. when integrating problems of viscoplasticity by use of the midpoint rule with $\alpha = 0.5$ we have the simple relation

$$\frac{\partial \mathbf{G}_k}{\partial \mathbf{Y}_{k-1}} = \frac{\partial \mathbf{G}_k}{\partial \mathbf{Y}_k} - 2\mathbf{I}, \tag{60}$$

and by use of the Euler-backward integration scheme we simply have

$$\frac{\partial \mathbf{G}_k}{\partial \mathbf{Y}_{k-1}} = -\mathbf{I}. \tag{61}$$

For problems of plasticity these results have to be slightly modified.

Term 4 This term is adopted from the previous time step. Thus it can be seen that the sensitivity analysis essentially yields a *recursion formula*. It is not necessary to take into account results from previous time steps.

Term 5 This term corresponds to the negative elasticity modulus $-\mathbf{C}$.

Term 6 Once the global ‘displacement vector’ $d\mathbf{V}_k/d\boldsymbol{\kappa}$ is known, we can deduce the ‘displacement vector’ $d\mathbf{v}_k^e/d\boldsymbol{\kappa}$ for each element, and it follows

$$\frac{d\boldsymbol{\varepsilon}_k}{d\boldsymbol{\kappa}} = \mathbf{B}_e \frac{d\mathbf{v}_k^e}{d\boldsymbol{\kappa}}, \tag{62}$$

where \mathbf{B}_e is the standard discrete strain matrix of the geometric linear theory.

Term 7 Here, the same remark as for Term 6 holds.

Let us return to the determination of the partial derivative of the stresses with respect to the material parameters i.e. $d^p \boldsymbol{\sigma}_k / d^p \boldsymbol{\kappa}$ in Eq. (54). This term is now easily obtained from Eqs. (55), (56) by *neglecting implicit derivatives of $\boldsymbol{\kappa}$ via the displacements $\hat{\mathbf{V}}_k(\boldsymbol{\kappa})$* . Consequently, it follows that:

$$\boxed{\frac{d^p \boldsymbol{\sigma}_k}{d^p \boldsymbol{\kappa}} = -\tilde{\mathbf{C}}_\sigma \left(\mathbf{h}_{1,k}^p - \frac{\partial \mathbf{g}_{1,k}}{\partial \mathbf{q}_k} \left[\frac{\partial \mathbf{g}_{2,k}}{\partial \mathbf{q}_k} \right]^{-1} \mathbf{h}_{2,k}^p \right)} \tag{63}$$

where

$$\begin{aligned}
 \mathbf{h}_{1,k}^p &:= \frac{\partial \mathbf{g}_{1,k}}{\partial \boldsymbol{\kappa}} + \frac{\partial \mathbf{g}_{1,k}}{\partial \mathbf{Y}_{k-1}} \frac{d\mathbf{Y}_{k-1}}{d\boldsymbol{\kappa}} + \frac{\partial \mathbf{g}_{1,k}}{\partial \boldsymbol{\varepsilon}_{k-1}} \frac{d\boldsymbol{\varepsilon}_{k-1}}{d\boldsymbol{\kappa}} \\
 \mathbf{h}_{2,k}^p &:= \frac{\partial \mathbf{g}_{2,k}}{\partial \boldsymbol{\kappa}} + \frac{\partial \mathbf{g}_{2,k}}{\partial \mathbf{Y}_{k-1}} \frac{d\mathbf{Y}_{k-1}}{d\boldsymbol{\kappa}} = \mathbf{h}_{2,k}
 \end{aligned} \tag{64}$$

REMARKS

- (1) The results (55), (56) and (63), (64) are identical to those obtained in [12], where a condensation of the internal variables was performed by reformulation of the state equation \mathbf{G}_k , rather than exploiting the structure of the local tangent moduli derived in Section 3.2.2.
- (2) Note, that the calculation of $d^p \boldsymbol{\sigma}_k / d^p \boldsymbol{\kappa}$ in Eqs. (63), (64) also necessitates the calculation of the derivative of state variables from the previous time step $d\mathbf{Y}_{k-1} / d\boldsymbol{\kappa}$, which is in contrast to problems of elasticity (see [14]).
- (3) Combining the results (39), (55), (56)₁ (63), (64)₁ the total derivative of the stresses can also be expressed as

$$\frac{d\boldsymbol{\sigma}_k}{d\boldsymbol{\kappa}} = \frac{d^p \boldsymbol{\sigma}_k}{d^p \boldsymbol{\kappa}} + \mathbf{C}_T \frac{d\boldsymbol{\varepsilon}_k}{d\boldsymbol{\kappa}} \tag{65}$$

Note the similarity of this expression to the total derivative of the residual in Eq. (52).

- (4) The main consequence of the solution strategy described in Section 4.2 is that the direct problem has to be solved many times for different material parameters. Consequently, it is important to use finite element approximations, which give accurate results with relatively low discretization. In this respect the assumed strain concept described by Simo/Rifai [29] proved to be very efficient. As noted in [29], standard stain driven integration algorithms can be applied within the assumed strain concept without further modifications. Furthermore, linearization is performed for an extended system of Eq. (22), which is solved by a condensation procedure (analogously to Lemma 1 of this work).

Now, it can be easily shown that analogous implications hold for the sensitivity analysis for solution of the inverse problem, where basically an extended system of Eq. (52) is solved by using the same condensation procedure as described in [29]. Furthermore, the results (55), (56) and (63), (64) carry over without any modification to the mixed finite element concept. Further details shall not be discussed in this paper.

4.4. Extension to plane stress problems

Concerning the sensitivity analysis for plane stress problems, basically an analogous procedure as described in Section 3.4 is performed. This is done by simple manipulation of $\partial \mathbf{G}_k / \partial \mathbf{Y}_k$ and $\partial \mathbf{G}_k / \partial \mathbf{Y}_{k-1}$ for the plane strain case with respect to the definition (44) for the vector of state variables. Note that $\partial \mathbf{G}_k / \partial \boldsymbol{\kappa}$ is not affected by this approach.

- Concerning $\partial \mathbf{G}_k / \partial \mathbf{Y}_k$, the last column of $\partial \mathbf{g}_{1,k} / \partial \boldsymbol{\sigma}_k$, i.e. $[\partial \mathbf{g}_{1,k} / \partial \boldsymbol{\sigma}_k]_{i,j=4}$ for the plane strain case is replaced by the vector \mathbf{b} defined in Eq. (46)₂. Furthermore, we have

$$\left[\frac{\partial \mathbf{g}_{2,k}}{\partial \boldsymbol{\sigma}_k} \right]_{i,j=4} = \mathbf{0}, \quad i = 1, \dots, 4. \tag{66}$$

- Concerning $\partial \mathbf{G}_k / \partial \mathbf{Y}_{k-1}$, we have

$$\left[\frac{\partial \mathbf{G}_k}{\partial \mathbf{Y}_{k-1}} \right]_{i,j=4} = \mathbf{0}, \quad i = 1, \dots, 4. \tag{67}$$

With this notation at hand the 3×1 partial load vector is determined according to Eq. (54) analogously to Eq. (48) where

$$\frac{d^p \sigma_k}{d^p \kappa} = - \left(\mathbf{A}_\sigma - \frac{1}{d_\sigma} \mathbf{b}_\sigma \otimes \mathbf{c}_\sigma \right) \left(\hat{\mathbf{h}}_{1,k}^p - \frac{\partial \mathbf{g}_{1,k}}{\partial \mathbf{q}_k} \left[\frac{\partial \mathbf{g}_{2,k}}{\partial \mathbf{q}_k} \right]^{-1} \hat{\mathbf{h}}_{2,k}^p \right). \quad (68)$$

Here, $\mathbf{A}_\sigma, \mathbf{b}_\sigma, \mathbf{c}_\sigma, d_\sigma$ are given in Eq. (47), and $\hat{\mathbf{h}}_{1,k}^p, \hat{\mathbf{h}}_{2,k}^p$ are modified expressions for the plane stress case of Eq. (64) as discussed above.

4.5. Remarks on computational aspects

- (1) The main significance of practical importance, that the sensitivity analysis yields a recursion formulae, is that determination of $dV_k/d\kappa$ can be performed *simultaneously* to the step-by-step solution of the direct problem. In this respect when solving the direct problem for a given set of parameters, three additional steps are necessary at the converged state of each time step: Firstly, the partial load vector (54) is determined in a *pre-processing procedure* with ‘stresses’ according to Eq. (63) at each quadrature point. Secondly, a linear system (53) is solved with a matrix \mathbf{K}_T already factorized at the converged state of the solution procedure for the direct problem. Thirdly, in a *post-processing procedure* an update of the total derivative of state variables $dY_k/d\kappa$ is performed at each quadrature point (in addition to the standard update procedure of state variables Y_k), compare the in-between loop in Fig. 1. For convenience, an overall structure for determination of the derivative of displacements with respect to material parameters for a given set of parameters κ obtained from the least-squares optimization procedure is summarized in Table 1.
- (2) From Fig. 1 it can be seen, that repeated solutions of the direct problem are necessary for varying parameter sets $\kappa^{(j)}, j = 0, 1, 2, \dots$. A reasonable reduction of the execution time (about 20%) for the identification process can be obtained, by storing the displacements at each time step, and using the vectors $U_k(\kappa^{(j-1)}), k = 1, \dots, N, j > 0$, as starting vectors for solution of the direct problem in the inner iteration loop for the actual parameter set $\kappa^{(j)}, j > 0$. If N is large, only every \bar{m} th vector is stored, where $\bar{m} > 0$ is some number, and the intermediate displacements are obtained by (linear) interpolation.
- (3) Concerning the gradient based optimization strategy for solution of problem (50) here only some basic ideas shall be presented. More details pertaining to mathematical issues can be found in [16, 17, 28, 36–39]. Concerning applications in the context of parameter identification we refer to [7, 8].

Table 1

Overall structure of the algorithm for determination of the derivative of displacements with respect to material parameters. Steps 3, 4 and 5 are the additional steps in the context of a standard FEM iteration procedure

-
- Step 1* OBTAIN set of material parameters κ from least-squares optimization procedure.
 INITIALIZE time step $k = 1$, vector of state variables, $Y_{k-1} = Y_0, dY_{k-1}/d\kappa = \mathbf{0}$
- Step 2* PERFORM standard FEM-Newton iteration for the direct problem and obtain
 (a) State variables $\hat{Y}_k(\kappa)$ by local iteration procedure at all quadrature points
 (b) Displacements $\hat{V}_k(\kappa)$ by global iteration procedure
- Step 3* PRE-PROCESSING: Determine partial load vector:
 (a) Calculate $d^p \sigma_k / d^p \kappa$ at all quadrature points
 (b) Assemble $d^p R_k / d^p \kappa = \mathbf{A}_{e-1}^{n, \text{dim}} \int_{\Omega_e} \mathbf{B}_e^T d^p \sigma_k / d^p \kappa d\Omega_e$
- Step 4* SOLVE linear system of equations
-

$$\frac{dV_k}{d\kappa} = -[\mathbf{K}_T]^{-1} \frac{d^p R_k}{d^p \kappa},$$

(with factorized matrix \mathbf{K}_T from the direct problem)

- Step 5* POST-PROCESSING: Update state variables $\hat{Y}_k(\kappa)$ and its derivatives $d\hat{Y}_k(\kappa)/d\kappa$
 IF k .eq. N , then EXIT
 else: Set $k \leftarrow k + 1$, GOTO 2.
-

The corresponding iteration scheme of a gradient-based projection algorithm for solution of Eq. (50) reads (see [16])

$$\boldsymbol{\kappa}^{(j+1)} = \mathcal{P} \left\{ \boldsymbol{\kappa}^{(j)} - \alpha^{(j)} \mathbf{H}^{(j)} \nabla f(\boldsymbol{\kappa}^{(j)}) \right\}, \quad j = 0, 1, 2, \dots \quad (69)$$

The projection operator \mathcal{P} is introduced, in order to take into account lower and upper bounds $a_i, b_i, i = 1, \dots, m$, for the material parameters and is defined as

$$\mathcal{P} \{ \boldsymbol{\kappa} \}_i := \min(\max(a_i, \kappa_i), b_i), \quad i = 1, \dots, m. \quad (70)$$

Furthermore, $\alpha^{(j)}$ is a step-length determined in a line search, which may be based on function evaluations (e.g. Armijo line-search). The iteration matrix $\mathbf{H}^{(j)}$ is a positive-definite iteration matrix such as the Gauss–Newton matrix or a BFGS matrix, which in the context of the above iteration scheme has to be ‘diagonalized’ (see [16] for an explanation of this terminology), in order to ensure descent properties of the iteration scheme. Concerning the specific update formula for \mathbf{H}_{BFGS} , we refer to [28] and to the modification due to Powell [40] in order to preserve positive-definiteness (see also Luenberger, p. 448). It is noteworthy, that for problems discussed in [8] we did numerical tests with the gradient method, i.e. $\mathbf{H}^{(j)} = \mathbf{I}^{m \times m}$, where $\mathbf{I}^{m \times m}$ is the identity, which in the context of the above iteration scheme (69) is known as the projected gradient method; however, this choice gave very poor results with respect to execution time. For more details on the algorithm such as scaling and indefinite iteration matrices we refer to [8, 17, 28, 36].

- (4) Lastly, the following side remark concerning problems in elasticity is noteworthy: For this kind of problems a post-processing procedure is not necessary, since as mentioned above, the calculation of $d^p \boldsymbol{\sigma}_k / d^p \boldsymbol{\kappa}$ is not dependent on the derivative of state variables from previous time steps.

5. Numerical examples

5.1. Cooks membrane problem

The first example intends to test our optimization algorithm of Section 4 in case of parameter re-identification for simulated data. We consider a tapered panel, clamped on one end and subjected to a shearing load on the other (see Fig. 2). The elastic version is known as ‘Cooks membrane problem’ in the literature. For spatial discretization of this problem the enhanced strain element as described in [29] is used. Here, it was shown that for non-linear computation based on J_2 -flow theory, practically, convergence is obtained with an 8×8 mesh.

Conceptually we proceed as follows: Firstly, a viscoplastic—direct—problem in plane strain is solved with assumed material data for the power law (12) with linear hardening (10) as shown in the third column of Table 2. Additionally, we assume $E = 1000$ and $\nu = 0.3$ for Youngs modulus and Poissons ratio, respectively. (Note, that units are not given here and below in order to describe the input data for material, loading and geometry for this purely numerical example.) The simulation is performed using load control, with load steps $\{F_k - F_{k-1}\}_{k=1}^5 = 0.5$ and $\{F_k - F_{k-1}\}_{k=6}^{10} = 1.0$, so that the total load is $F = 7.5$. The $N = 10$ time steps for integration are chosen as $\{t_k - t_{k-1}\}_{k=1}^5 = 1.0$ and $\{t_k - t_{k-1}\}_{k=6}^{10} = 0.5$, so that the total time is $T = 7.5$. The resulting final deformed configuration is plotted in Fig. 2, and the resulting vertical top corner displacement parameters is plotted against the load factor in Fig. 3 (Solution). For re-identification we use data for the u_x and u_y -displacements at $n_{mp} = 15$ arbitrary chosen points $\{\mathbf{x}_i\}_{i=1}^{n_{mp}}$ as shown in Fig. 2.

As an objective function the following scaled least-squares function is examined

$$f(\boldsymbol{\kappa}) = \sum_{k=1}^{n_{\text{dat}}=10} \sum_{i=1}^{m_p=15} \sum_{l=1}^{n_{\text{dim}}=2} \left(\frac{u_{lik} - \bar{u}_{lik}}{u_{lik}^{(j=0)} - \bar{u}_{lik}} \right)^2 \rightarrow \min_{\boldsymbol{\kappa}}, \quad (71)$$

where $u_{lik} := u_l(\mathbf{x}_i, t_k)$, and the upper index $(\bullet)^{(j)}$ refers to the iteration number of the identification process. For optimization the projection algorithm due to Bertsekas [16] combined with a BFGS update

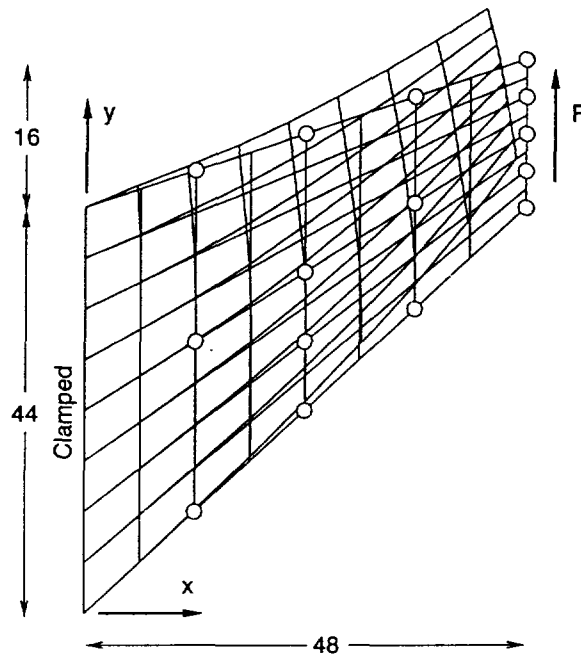


Fig. 2. Cooks membrane problem: Geometry, discretization, final deformed configuration and position of nodal points for re-identification of parameters of a viscoplastic power law. The final load is $F = 7.5$.

Table 2

Cooks membrane problem: Starting, target and obtained values of the optimization process for the material parameters of a viscoplastic power law

	Starting	Target	Obtained
n'	1.0	8.0	8.0
K'	1.0	0.8	0.8
H	1.0	4.5	4.5
σ_0	1.0	0.25	0.25

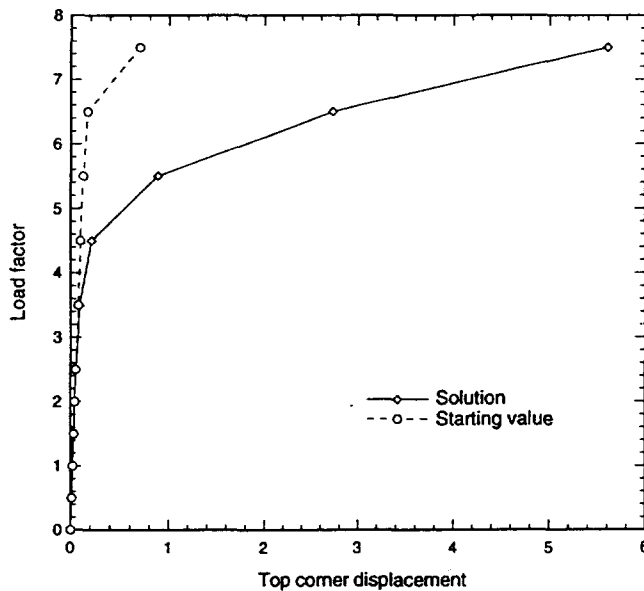


Fig. 3. Cooks membrane problem: vertical top corner displacement versus load factor for two different sets of material parameters for a viscoplastic power law.

scheme [17] is applied. The starting vector for the optimization process is given in the second column of Table 2. The corresponding top corner displacement versus load factor is also shown in Fig. 3 (starting value). From the fourth column of Table 2 it can be seen, that at the solution point all 5 parameters of the power law were re-identified.

In Fig. 4 the scaled objective function (71) is plotted against the number of iterations. It can be seen that convergence at the beginning of the identification process is very slow. Near the solution point convergence is obtained at a superlinear rate, which is typical for Quasi-Newton methods, however which in general cannot be obtained by zero-order methods such as an evolutionary strategy.

5.2. Compact tension specimen

The second example is concerned with a compact tension specimen with geometry as shown in Fig. 5. For this example experimental data were generated with a grating method in the context of the german research network Sonderforschungsbereich 319 (SFB 319): ‘Stoffgesetze für das inelastische Verhalten metallischer Werkstoffe–Entwicklung und Anwendung’ in collaboration with 3 departments from the University of Braunschweig, Germany. In particular, the actual experiment was performed at the Institut für Stahlbau. Simultaneously optical measurements were performed by the Institut für experimentelle Mechanik, and these data were analyzed using digital equipments at the Mechanik-Zentrum.

The material of the specimen is a mild steel, Baustahl St52 due to the german specifications for construction steel. Concerning the elastic constants we set $E = 20600 \text{ kN/cm}^2$ and $\nu = 0.3$ for Youngs modulus and Poissons ratio, respectively. A force is submitted to a pin, which is inserted at the lower hole of the sample, whilst the upper hole is fixed, also by a pin. The load is increased with a constant rate of 2 kN/min. The fixation of the sample during the experiment is shown in a photograph in Fig. 6. Note that failure of the sample occurred at a load of 132 kN, so that we will consider a maximal load seize of 118 kN for the following simulation.

For experimental determination of the displacements gratings are positioned on the surface. These gratings are photographed with digital cameras at consecutive load steps as shown in Table 3 [41]. Then, it is possible to determine grid coordinates by use of correlation filters [42] with an accuracy of ± 0.1

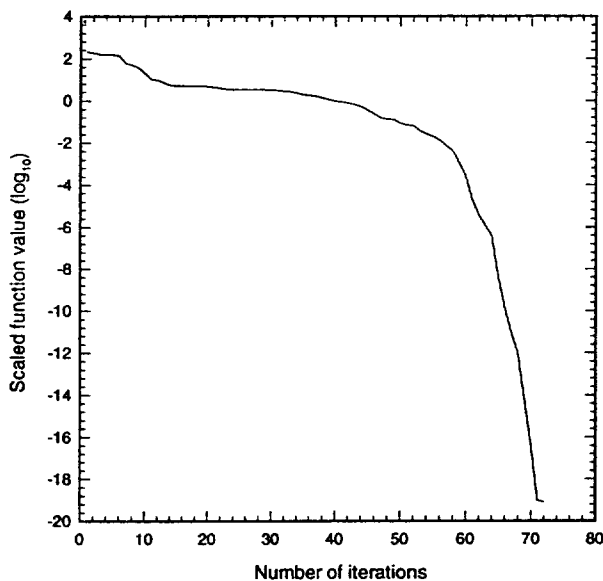


Fig. 4. Cooks membrane problem: Iteration behaviour of the Bertsekas algorithm for the scaled least-squares function value for re-identification of parameters of a viscoplastic power model.

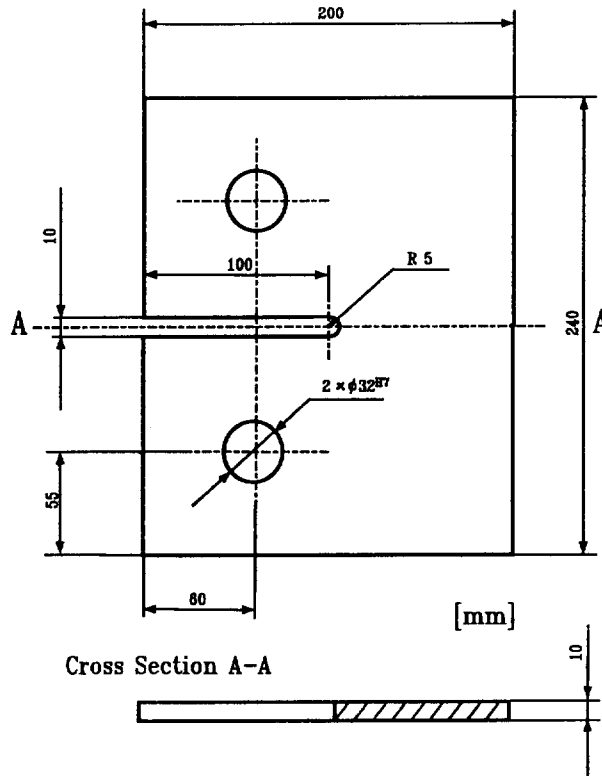


Fig. 5. Compact tension specimen: Geometry of the sample.

pixel. If, e.g. the distance of the grid lines is 20 pixel, this ensues a scattering for the strains of $\pm 0.1/20 = \pm 0.005$. By use of a smoothing technique this value can be reduced to ± 0.001 . Therefore, this grid technique is most suitable to measure plastic strains which are in the range of more than one percent.

For numerical simulation of the direct problem the assumed strain method as described in [29] is used. The spatial discretization for this plane stress problem is shown in Fig. 7. Time integration is performed with the Euler backward rule in 33 load steps. For modeling of the inelastic material behaviour J_2 -flow theory is considered with both, linear and non-linear isotropic hardening according to Eqs. (8) and (10), respectively.

As input data for the identification process we used u - and/or v -displacements at different, arbitrarily chosen points as shown in Fig. 7, so that the total number of data at each time step $t_j, j = 1, \dots, n_{\text{dat}} = 17$ is $n_{\text{xdat}} = 22$. In this respect, the following objective function of least-squares type without weighting factors is examined

$$f(\boldsymbol{\kappa}) = \sum_{i=1}^{n_{\text{dat}}=17} \sum_{j=1}^{n_{\text{xdat}}=22} (u_{ij} - \bar{u}_{ij})^2 \longrightarrow \min_{\boldsymbol{\kappa}}, \quad (72)$$

where here u_{ij} denotes the direction for the displacement in either x - or y -direction. As for the previous example, the numerical tool for minimizing the problem (72) is the Bertsekas algorithm as described in [16, 17].

In Table 4 the results of six different runs are compared: In Run 1 to Run 3 the effect of different starting values and the effect of perturbed experimental data is considered for the linear kinematic rule,